Longitudinal Dynamics and Adaptive Control Application for an Aeroelastic Generic Transport Model

Nhan Nguyen*
NASA Ames Research Center, Moffett Field, CA 94035
Ilhan Tuzcu†
California State University, Sacramento, CA 95819
Tansel Yucelen‡ and Anthony Calise§
Georgia Institute of Technology, Atlanta, GA 30332

This paper presents an aeroelastic model of longitudinal dynamics of a generic transport model (GTM). Aeroelasticity theory is used to develop an aeroelastic flight dynamic model of the flexible GTM to account for interactions between wing bending and torsion on aircraft performance and stability. The Galerkin's method is used to implement a weak-form solution of the aeroelastic equations of the aircraft. The weak-form aeroelastic equations are then coupled with the longitudinal dynamic equations of the rigid-body aircraft to formulate an aeroelastic flight dynamic model. This model is then used to create a reduced-order state space model of the rigid-body longitudinal dynamics with the flexible-body dynamics represented as unmodeled dynamics. Matched uncertainty and wind gust disturbances are introduced in the model and is effectively addressed by two recently developed robust modification adaptive control methods: Optimal Control Modification and Adaptive Loop Recovery. Both methods demonstrate the effectiveness in reducing the effects of the uncertainty and wind gust disturbances.

I. Introduction

Light weight aircraft design has received a considerable attention in recent years as a means for improving cruise efficiency. Reducing aircraft weight results in lower lift requirement which directly translates into lower induced drag, hence reduced engine thrust requirement during cruise. The use of light-weight materials such as advanced composite materials has been adopted by airframe manufacturers in a number of current and future aircraft. Modern light-weight materials can provide less structural rigidity while maintaining sufficient load-carrying capacity. As structural flexibility increases, aeroelastic interactions with aerodynamic forces and moments become an increasingly important consideration in aircraft design. Understanding aeroelastic effects can improve the prediction of aircraft aerodynamic performance and provide an insight into how to design an aerodynamically efficient airframe that exhibits a high degree of flexibility. Moreover, structural flexibility of airframes can cause significant aeroelastic interactions that can degrade vehicle stability margins, potentially leading to loss of control. There exists a trade-off between the desire of having light weight, flexible structures for weight savings and the need for maintaining sufficient robust stability margins from aeroelastic instability.

This paper describes an aeroelastic model of a generic transport model (GTM). The aeroelastic model is based on one-dimensional structural dynamic theory that models a wing structure as a one-dimensional elastic member in a combined coupled bending-torsion motion. Aeroelastic analysis is performed based on the quasi-steady state aerodynamic assumption. Flight control simulations of aircraft response to gust loads are performed. Two adaptive control schemes based on the optimal control modification[1] and adaptive loop recovery[2] are designed as adaptive augmentation controllers to demonstrate the effectiveness of gust load alleviation and uncertainty accommodation using adaptive control.

*Research Scientist, Associate Fellow AIAA, Intelligent Systems Division, nhan.t.nguyen@nasa.gov
†Assistant Professor, AIAA Senior Member, Mechanical Engineering Department, tuzcui@ecs.csus.edu
‡Graduate Research Assistant, Student Member AIAA, School of Aerospace Engineering, tansel@gatech.edu
§Professor, Fellow Member AIAA, School of Aerospace Engineering, anthony.calise@aerospace.gatech.edu

II. Aeroelastic Flight Dynamic Modeling

The aeroelastic effects of the generic transport model (GTM) is assumed to be contributed only by the wing structures. Fuselage and tail surface deflections are assumed to be negligible. For this study, aeroelasticity theory is used to develop an aeroelastic flight dynamic model of the GTM to account for interactions between wing bending and torsion on aircraft performance and stability only in the pitch axis. Future work will extend the analysis to the other axes.

A. Reference Frames

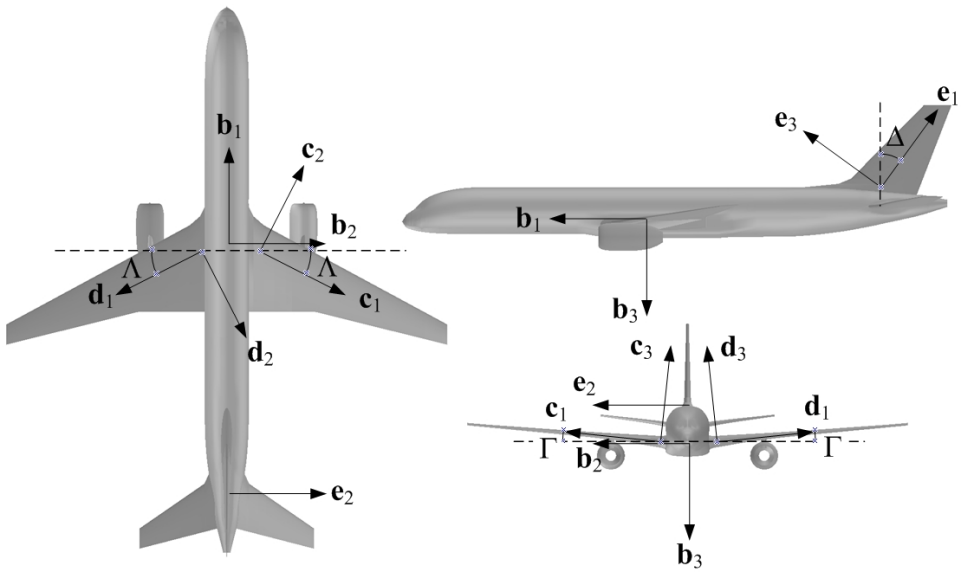

Figure 1 - Aircraft Reference Frames

Figure 1 illustrates three orthogonal views of a typical aircraft. Several reference frames are introduced to facilitate the rigid-body dynamic and structural dynamic analysis of the lifting surfaces. For example, the aircraft inertial reference frame A is defined by unit vectors $\mathbf{a}_1$, $\mathbf{a}_2$, and $\mathbf{a}_3$ fixed to the non-rotating earth. The aircraft body-fixed reference frame B is defined by unit vectors $\mathbf{b}_1$, $\mathbf{b}_2$, and $\mathbf{b}_3$. The reference frames A and B are related by three successive rotations: 1) the first rotation about $\mathbf{a}_3$ by the heading angle ψ that results in an intermediate reference frame $A^{'}$ defined by unit vectors $\mathbf{a}_1^{'}$, $\mathbf{a}_2^{'}$, and $\mathbf{a}_3^{'}$ (not shown), 2) the second rotation about $\mathbf{a}_2^{'}$ by the pitch angle θ that results in an intermediate reference frame $B^{'}$ defined by unit vectors $\mathbf{b}_1^{'}$, $\mathbf{b}_2^{'}$, and $\mathbf{b}_3^{'}$ (not shown), and 3) the third rotation about $\mathbf{b}_1^{'}$ by the bank angle ϕ that results in the reference frame B. This relationship can be expressed as

$$\begin{bmatrix} \mathbf{a}_1 \\ \mathbf{a}_2 \\ \mathbf{a}_3 \end{bmatrix} = \begin{bmatrix} \cos\psi & -\sin\psi & 0 \\ \sin\psi & \cos\psi & 0 \\ 0 & 0 & 1 \end{bmatrix} \begin{bmatrix} \cos\theta & 0 & \sin\theta \\ 0 & 1 & 0 \\ -\sin\theta & 0 & \cos\theta \end{bmatrix} \begin{bmatrix} 1 & 0 & 0 \\ 0 & \cos\phi & -\sin\phi \\ 0 & \sin\phi & \cos\phi \end{bmatrix} \begin{bmatrix} \mathbf{b}_1 \\ \mathbf{b}_2 \\ \mathbf{b}_3 \end{bmatrix}$$
$$= \begin{bmatrix} \cos\psi\cos\theta & -\sin\psi\cos\phi + \cos\psi\sin\theta\sin\phi & \sin\psi\sin\phi + \cos\psi\sin\theta\cos\phi \\ \sin\psi\cos\theta & \cos\psi\cos\phi + \sin\psi\sin\theta\sin\phi & -\cos\psi\sin\phi + \sin\psi\sin\theta\cos\phi \\ -\sin\theta & \cos\theta\sin\phi & \cos\theta\cos\phi \end{bmatrix} \begin{bmatrix} \mathbf{b}_1 \\ \mathbf{b}_2 \\ \mathbf{b}_3 \end{bmatrix} \tag{1}$$

The left wing elastic reference frame D is defined by unit vectors $\mathbf{d}_1$, $\mathbf{d}_2$, and $\mathbf{d}_3$. The reference frames B and D are related by three successive rotations: 1) the first rotation about $\mathbf{b}_3$ by the elastic axis sweep angle $\frac{\pi}{2} + \Lambda$ that results in an intermediate reference frame $B^{''}$ defined by unit vectors $\mathbf{b}_1^{''}$, $\mathbf{b}_2^{''}$, and $\mathbf{b}_3^{''}$ (not shown), 2) the second rotation about $\mathbf{b}_2^{''}$ by the elastic axis dihedral angle Γ that results in an intermediate reference frame $D^{'}$ defined by unit vectors $\mathbf{d}_1^{'}$, $\mathbf{d}_2^{'}$, and $\mathbf{d}_3^{'}$ (not shown), and 3) the third rotation about $\mathbf{d}_1^{'}$ by an angle π that results in the reference frame D. This

relationship can be expressed as

$$\begin{bmatrix} \mathbf{b}_1 \\ \mathbf{b}_2 \\ \mathbf{b}_3 \end{bmatrix} = \begin{bmatrix} -\sin\Lambda & \cos\Lambda & 0 \\ -\cos\Lambda & -\sin\Lambda & 0 \\ 0 & 0 & 1 \end{bmatrix} \begin{bmatrix} \cos\Gamma & 0 & \sin\Gamma \\ 0 & 1 & 0 \\ -\sin\Gamma & 0 & \cos\Gamma \end{bmatrix} \begin{bmatrix} 1 & 0 & 0 \\ 0 & -1 & 0 \\ 0 & 0 & -1 \end{bmatrix} \begin{bmatrix} \mathbf{d}_1 \\ \mathbf{d}_2 \\ \mathbf{d}_3 \end{bmatrix}$$
$$= \begin{bmatrix} -\sin\Lambda\cos\Gamma & -\cos\Lambda & \sin\Lambda\sin\Gamma \\ -\cos\Lambda\cos\Gamma & \sin\Lambda & \cos\Lambda\sin\Gamma \\ -\sin\Gamma & 0 & -\cos\Gamma \end{bmatrix} \begin{bmatrix} \mathbf{d}_1 \\ \mathbf{d}_2 \\ \mathbf{d}_3 \end{bmatrix} \tag{2}$$

Generally, the effect of the dihedral angle can be significant. A full analysis with the dihedral angle can be performed but can also result in a very complex analytical formulation. Thus, to simplify the analysis, the dihedral effect is assumed to be negligible in this study. The right wing reference frame C can be established in a similar manner. In the analysis, the aeroelastic effects on the fuselage, horizontal stabilizers, and vertical stabilizer are not considered, but the analytical method can be formulated for analyzing these lifting surfaces if necessary. In general, a whole aircraft analysis approach should be conducted to provide a comprehensive assessment of the effect of structural flexibility on aircraft performance and stability. However, the scope of this study pertains to only the wing structures.

B. Elastic Analysis

In the subsequent analysis, the combined motion of the left wing is considered. The motion of the right wing is a mirror image of that of the left wing for symmetric flight. The wing has a varying pre-twist angle $\gamma(x)$ commonly designed in many aircraft. Typically, the wing pre-twist angle varies from being nose-up at the wing root to nose-down at the wing tip. The nose-down pre-twist at the wing tip is designed to delay stall onsets. This is called a wash-out twist distribution. Under aerodynamic forces and moments, the aeroelastic deflections of a wing introduce stresses and strains into the wing structure. The internal structure of a wing typically comprises a complex arrangement of load carrying spars and wing boxes. Nonetheless, the elastic behavior of a wing can be captured by the use of equivalent stiffness properties. These properties can be derived from structural certification testing that yields information about wing deflections as a function of loading. For high aspect ratio wings, an equivalent one-dimensional elastic approach can be used to analyze aeroelastic deflections with good accuracy. The equivalent one-dimensional elastic approach is a typical formulation in many aeroelasticity studies.[3] It is assumed that the effect of wing curvature is ignored and the one-dimensional aeroelasticity theory is used to model the wing aeroelastic deflections.

Consider an airfoil section on the left wing as shown in Figure 2 undergoing bending and twist deflections.

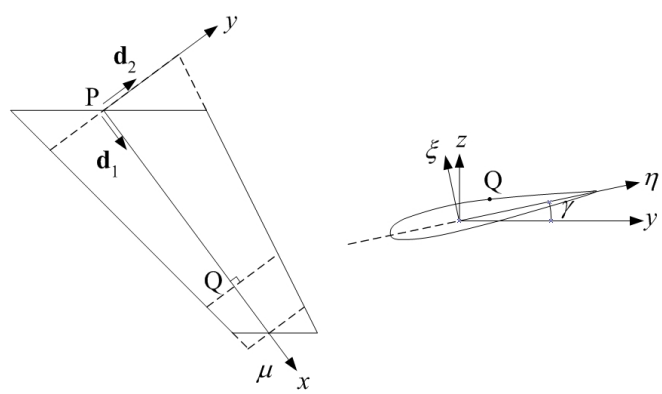

Figure 2 - Left Wing Reference Frame

Let (x, y, z) be the coordinates of a point Q on the airfoil. Then the undeformed local airfoil coordinates of point Q are

$$\begin{bmatrix} y \\ z \end{bmatrix} = \begin{bmatrix} \cos\gamma & -\sin\gamma \\ \sin\gamma & \cos\gamma \end{bmatrix} \begin{bmatrix} \eta \\ \xi \end{bmatrix} \tag{3}$$

where η and ξ are local airfoil coordinates, and γ is the wing section pre-twist angle, positive nose-down.[4]

Then differentiating with respect to x gives

$$\begin{bmatrix} y_x \\ z_x \end{bmatrix} = \gamma' \begin{bmatrix} -\sin\gamma & -\cos\gamma \\ \cos\gamma & -\sin\gamma \end{bmatrix} \begin{bmatrix} \eta \\ \xi \end{bmatrix} = \begin{bmatrix} -z\gamma' \\ y\gamma' \end{bmatrix} \tag{4}$$

The axial or extensional deflection of a wing is generally very small and therefore can usually be neglected. Let Θ be a torsional twist angle about the x-axis, positive nose-down, and let W and V be flapwise and chordwise bending deflections of point Q, respectively.. Then, the rotation angle due to the elastic deformation can be expressed as

$$\phi(x,t) = \Theta\mathbf{d}_1 - W_x\mathbf{d}_2 + V_x\mathbf{d}_3 \tag{5}$$

where the subscripts x and t denote the partial derivatives of Θ, W, and V.

Let (x_1, y_1, z_1) be the coordinates of point Q on the airfoil in the reference frame D. Then the coordinates (x_1, y_1, z_1) are computed using the small angle approximation as

$$\begin{bmatrix} x_1(x,t) \\ y_1(x,t) \\ z_1(x,t) \end{bmatrix} = \begin{bmatrix} x \\ y+V \\ z+W \end{bmatrix} + \begin{bmatrix} \phi \times (y\mathbf{d}_2 + z\mathbf{d}_3).\mathbf{d}_1 \\ \phi \times (y\mathbf{d}_2 + z\mathbf{d}_3).\mathbf{d}_2 \\ \phi \times (y\mathbf{d}_2 + z\mathbf{d}_3).\mathbf{d}_3 \end{bmatrix} = \begin{bmatrix} x - yV_x - zW_x \\ y + V - z\Theta \\ z + W + y\Theta \end{bmatrix} \tag{6}$$

Differentiating x_1, y_1, and z_1 with respect to x yields

$$\begin{bmatrix} x_{1,x} \\ y_{1,x} \\ z_{1,x} \end{bmatrix} = \begin{bmatrix} 1 - yV_{xx} + z\gamma' V_x - zW_{xx} - y\gamma' W_x \\ -z\gamma' + V_x - z\Theta_x - y\gamma'\Theta \\ y\gamma' + W_x + y\Theta_x - z\gamma'\Theta \end{bmatrix} \tag{7}$$

Neglecting the transverse shear effect, the longitudinal strain is computed as[5]

$$\varepsilon = \frac{ds_1 - ds}{ds} = \frac{s_{1,x}}{s_x} - 1 \tag{8}$$

where

$$s_x = \sqrt{1 + y_x^2 + z_x^2} = \sqrt{1 + (y^2+z^2)(\gamma')^2} \tag{9}$$

$$s_{1,x} = \sqrt{x_{1,x}^2 + y_{1,x}^2 + z_{1,x}^2} = \sqrt{1 + (y^2+z^2)(\gamma')^2 - 2yV_{xx} - 2zW_{xx} + 2(y^2+z^2)\gamma'\Theta_x} \tag{10}$$

For a small wing twist angle γ, the longitudinal strain is obtained as

$$\varepsilon = -yV_{xx} - zW_{xx} + (y^2+z^2)\gamma'\Theta_x \tag{11}$$

The moments acting on the wing are then obtained as

$$\begin{aligned} \begin{bmatrix} M_x \\ M_y \\ M_z \end{bmatrix} &= \begin{bmatrix} GJ\Theta_x \\ 0 \\ 0 \end{bmatrix} + \iint E\varepsilon \begin{bmatrix} (y^2+z^2)(\gamma' + \Theta_x) \\ -z \\ -y \end{bmatrix} dydz \\ &= \begin{bmatrix} GJ + EB_1(\gamma')^2 & -EB_2\gamma' & -EB_3\gamma' \\ -EB_2\gamma' & EI_{yy} & -EI_{yz} \\ -EB_3\gamma' & -EI_{yz} & EI_{zz} \end{bmatrix} \begin{bmatrix} \Theta_x \\ W_{xx} \\ V_{xx} \end{bmatrix} \end{aligned} \tag{12}$$

where E is the Young's modulus; G is the shear modulus; γ' is the derivative of the wing pre-twist angle; I_{yy}, I_{yz}, and I_{zz} are the section area moments of inertia about the flapwise axis; J is the torsional constant; and B_1, B_2, and B_3 are the bending-torsion coupling constants which are defined as

$$\begin{bmatrix} B_1 \\ B_2 \\ B_3 \end{bmatrix} = \iint (y^2+z^2) \begin{bmatrix} y^2+z^2 \\ z \\ y \end{bmatrix} dydz \tag{13}$$

The strain analysis shows that for a pre-twisted wing the bending deflections W and V are coupled to the torsional deflection Θ via the slope of the wing pre-twist angle. This coupling can be significant if the term γ' is dominant as in highly twisted wings such as turbomachinery blades. For an aircraft wing structure, a simplification can be made by neglecting the chordwise bending deflection. Thus, the resulting moments are now given as

$$\begin{bmatrix} M_x \\ M_y \end{bmatrix} = \begin{bmatrix} GJ + EB_1\left(\gamma'\right)^2 & -EB_2\gamma' \\ -EB_2\gamma' & EI_{yy} \end{bmatrix} \begin{bmatrix} \Theta_x \\ W_{xx} \end{bmatrix} \tag{14}$$

C. Aeroelastic Angle of Attack

The relative velocity of the air approaching a wing section includes the contribution from the wing elastic deflection that results in changes in the local angle of attack. Since aerodynamic forces and moments are dependent on the local angle of attack, the wing aeroelastic deflections will generate additional elastic forces and moments. The local angle of attack depends on the relative approaching air velocity as well as the rotation angle ϕ from Eq. (5). The relative air velocity in turn also depends on the deflection-induced velocity. The local velocity components at point Q in the reference frame D are given by[4]

$$\begin{bmatrix} v_x \\ v_y \\ v_z \end{bmatrix} = \begin{bmatrix} -u\sin\Lambda + x_{1,t} \\ -u\cos\Lambda + y_{1,t} \\ -w - qx_a + z_{1,t} \end{bmatrix} = \begin{bmatrix} -u\sin\Lambda - zW_{xt} \\ -u\cos\Lambda - z\Theta_t \\ -w - qx_a + W_t + y\Theta_t \end{bmatrix} \tag{15}$$

where $u \approx V_\infty$, $w \approx V_\infty\alpha$, q is the aircraft pitch rate, x_a is the position of point Q with respect to the aircraft C.G. (positive aft of C.G.) measured in the aircraft reference frame B, and y and z are coordinates of point Q in the reference frame D.

In order to compute the aeroelastic forces and moments, the velocity must be transformed from the reference frame D to the airfoil local coordinate reference frame defined by (μ, η, ξ) as shown in Figure 2. Then the transformation can be performed using two successive rotation matrix multiplication operations as

$$\begin{aligned} \begin{bmatrix} v_\mu \\ v_\eta \\ v_\xi \end{bmatrix} &= \begin{bmatrix} 1 & 0 & 0 \\ 0 & \cos(\Theta+\gamma) & \sin(\Theta+\gamma) \\ 0 & -\sin(\Theta+\gamma) & \cos(\Theta+\gamma) \end{bmatrix} \begin{bmatrix} \cos W_x & 0 & \sin W_x \\ 0 & 1 & 0 \\ -\sin W_x & 0 & \cos W_x \end{bmatrix} \begin{bmatrix} v_x \\ v_y \\ v_z \end{bmatrix} \\ &= \begin{bmatrix} v_x\cos W_x + v_z\sin W_x \\ -v_x\sin W_x\sin(\Theta+\gamma) + v_y\cos(\Theta+\gamma) + v_z\cos W_x\sin(\Theta+\gamma) \\ -v_x\sin W_x\cos(\Theta+\gamma) - v_y\sin(\Theta+\gamma) + v_z\cos W_x\cos(\Theta+\gamma) \end{bmatrix} \end{aligned} \tag{16}$$

For small deflections, the local velocity components can be simplified as

$$\begin{bmatrix} v_\mu \\ v_\eta \\ v_\xi \end{bmatrix} = \begin{bmatrix} v_x + v_z W_x \\ v_y + v_z(\Theta+\gamma) \\ v_z - v_x W_x - v_y(\Theta+\gamma) \end{bmatrix} \tag{17}$$

Referring to Figure 3, the local aeroelastic angle of attack on the airfoil section due to the velocity components v_η and v_ξ in the reference frame D is computed as

$$\alpha_c = \frac{v_\xi}{v_\eta} = \frac{\bar{v}_\xi + \Delta v_\xi}{\bar{v}_\eta + \Delta v_\eta} \tag{18}$$

where

$$\bar{v}_\xi = -w - qx_a \tag{19}$$

$$\bar{v}_\eta = -u\cos\Lambda \tag{20}$$

$$\Delta v_\xi = W_t + y\Theta_t - v_x W_x - v_y(\Theta+\gamma) \tag{21}$$

$$\Delta v_\eta = -z\Theta_t + v_z(\Theta+\gamma) \tag{22}$$

Then the local aeroelastic angle of attack can be evaluated as

$$\alpha_c = \frac{v_\xi}{\bar{v}_\eta} - \frac{\bar{v}_\xi \Delta v_\eta}{\bar{v}_\eta^2} = \frac{-w - qx_a + W_t + y\Theta_t - v_x W_x - v_y(\Theta+\gamma)}{-u\cos\Lambda} - \frac{(-w - qx_a)\left[-z\Theta_t + v_z(\Theta+\gamma)\right]}{u^2\cos^2\Lambda} \tag{23}$$

Ignoring the nonlinear terms, the expression for the local aeroelastic angle of attack is obtained as[4]

$$\alpha_c(x,y,z) = \frac{\alpha}{\cos\Lambda} + \frac{qx_a}{V_\infty\cos\Lambda} - \gamma(x) - W_x\tan\Lambda - \Theta - \frac{W_t + y\Theta_t}{V_\infty\cos\Lambda} - \frac{(w+qx_a)\left[z\Theta_t + (w+qx_a)(\Theta+\gamma)\right]}{V_\infty^2\cos^2\Lambda} \tag{24}$$

The terms W_t and Θ_t contribute to aerodynamic damping forces which can be significant for aeroelastic stability.

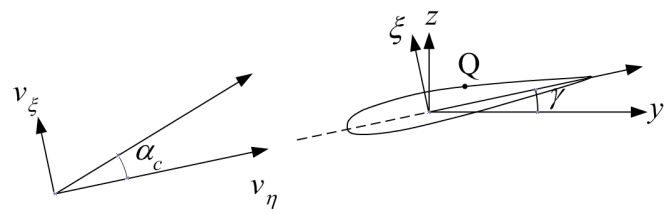

Figure 3 - Airfoil Local Coordinates

For aeroelastic analysis, the steady state aerodynamic method assumes that the steady state lift circulation occurs at the aerodynamic center of the oscillating airfoil, which may be taken to be the quarter-point. On the other hand, the unsteady aerodynamic method assumes that the unsteady circulation acts at the $3/4$-chord point.[4] Both Theodorsen's method for simple harmonic airfoil motion[6] and Peters' finite-state method can be used to analyze unsteady aerodynamics.[3] Based on the steady state aerodynamic assumption, the local angle of attack of an airfoil section at the elastic axis is evaluated at $y = -e$ and $z = 0$. Neglecting the last term, the expression for α_c is

$$\alpha_c(x) = \frac{\alpha}{\cos\Lambda} + \frac{qx_{ac}}{V_\infty\cos\Lambda} - \gamma(x) - W_x\tan\Lambda - \Theta - \frac{W_t - e\Theta_t}{V_\infty\cos\Lambda} \tag{25}$$

where x_{ac} is the distance from aircraft C.G. to the aerodynamic center measured in aircraft reference frame B (positive aft of C.G.) e is the distance between the aerodynamic center and the elastic axis.

For unsteady aerodynamics, the local angle of attack is evaluated at $y = b\left(\frac{1}{2} - a\right)$

$$\alpha_c = \frac{\alpha}{\cos\Lambda} + \frac{qx_{ac}}{V_\infty\cos\Lambda} - \gamma(x) - W_x\tan\Lambda - \Theta - \frac{W_t + b\left(\frac{1}{2}-a\right)\Theta_t}{V_\infty\cos\Lambda} \tag{26}$$

where b is the half-chord length and $-1 \le a \le 1$ is a parameter such that the elastic axis is located at a distance $-ab$ from the mid-chord and $a < 0$ when the elastic axis is forward of the mid-chord.

D. Wing Aeroelasticity

The equilibrium conditions for bending and torsion are expressed as

$$\frac{\partial M_x}{\partial x} = -m_x \tag{27}$$

$$\frac{\partial^2 M_y}{\partial x^2} = f_z - \frac{\partial m_y}{\partial x} \tag{28}$$

where m_x is the pitching moment per unit span about the elastic axis, f_z is the lift force per unit span, and m_y is the bending moment per unit span about the flapwise axis of the wing which is assumed to be zero.

The local lift coefficients and pitching moment are given by

$$c_L(x) = c_{L_0} + c_{L_\alpha}\alpha_c(x) + c_{L_\delta}\delta \tag{29}$$

$$c_m(x) = c_{m_{ac}} + \frac{e}{c}\left[c_{L_0} + c_{L_\alpha}\alpha_c(x)\right] + \sum_{k=1}^{m}\left(c_{m_{\delta_k}} + \frac{e}{c}c_{L_{\delta_k}}\right)\delta_k \tag{30}$$

where $c_{m_{ac}}$ is the section pitching moment coefficient about the section at the aerodynamic center, c_{L_0} is the section lift coefficient at zero angle of attack, c_{L_α} is the section lift vs. angle of attack curve slope, c is the section chord, δ_k is the surface deflection of the k-th flap, and $c_{L_{\delta_k}}$ and $c_{m_{\delta_k}}$ are the section lift and pitching moment control derivative at the quarter-chord point due to the k-th flap.

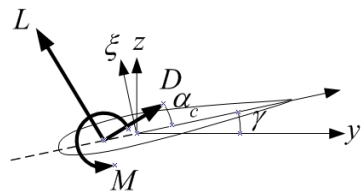

Figure 4 - Airfoil Forces and Moment

Using the sign convention as shown in Figure 4, the lift force and pitching moment per unit span can be expressed as

$$f_z = \left[c_{L_0} + c_{L_\alpha}\left(\frac{\alpha}{\cos\Lambda} + \frac{qx_{ac}}{V_\infty\cos\Lambda} - \gamma - W_x\tan\Lambda - \Theta - \frac{W_t - e\Theta_t}{V_\infty\cos\Lambda}\right) + \sum_{k=1}^{m} c_{L_{\delta_k}}\delta_k\right] q_\infty\cos^2\Lambda c - \rho g A - \rho A W_{tt} + \rho A e_{cg}\Theta_{tt} \quad (31)$$

$$m_x = -\left\{\frac{c}{e}c_{m_{ac}} + \left[c_{L_0} + c_{L_\alpha}\left(\frac{\alpha}{\cos\Lambda} + \frac{qx_{ac}}{V_\infty\cos\Lambda} - \gamma - W_x\tan\Lambda - \Theta - \frac{W_t - e\Theta_t}{V_\infty\cos\Lambda}\right) + \sum_{k=1}^{m}\left(\frac{c}{e}c_{m_{\delta_k}} + c_{L_{\delta_k}}\right)\delta_k\right]\right\} \times e q_\infty\cos^2\Lambda c + \rho g A e_{cg} - \rho I_{xx}\Theta_{tt} + \rho A e_{cg} W_{tt} \quad (32)$$

where q_∞ is the dynamic pressure, ρ is the wing material density including fuel density, A is the cross sectional area of a wing section, e_{cg} is the eccentricity between the center of mass and the elastic axis (positive corresponding to the center of mass located forward of the elastic axis), I_{xx} is the section polar area moment of inertia, and the term $\cos^2\Lambda$ accounts for the wing sweep angle Λ as measured from the elastic axis.

The bending and torsion aeroelastic equations then become

$$\frac{\partial^2}{\partial x^2}\left(-EB_2\gamma'\Theta_x + EI_{yy}W_{xx}\right) = \left[c_{L_0} + c_{L_\alpha}\left(\frac{\alpha}{\cos\Lambda} + \frac{qx_{ac}}{V_\infty\cos\Lambda} - \gamma - W_x\tan\Lambda - \Theta - \frac{W_t - e\Theta_t}{V_\infty\cos\Lambda}\right) + \sum_{k=1}^{m} c_{L_{\delta_k}}\delta_k\right] q_\infty\cos^2\Lambda c - \rho g A - \rho A W_{tt} + \rho A e_{cg}\Theta_{tt} \quad (33)$$

$$\frac{\partial}{\partial x}\left\{\left[GJ + EB_1\left(\gamma'\right)^2\right]\Theta_x - EB_2\gamma' W_{xx}\right\} = \left\{\frac{c}{e}c_{m_{ac}} + \left[c_{L_0} + c_{L_\alpha}\left(\frac{\alpha}{\cos\Lambda} + \frac{qx_{ac}}{V_\infty\cos\Lambda} - \gamma - W_x\tan\Lambda - \Theta - \frac{W_t - e\Theta_t}{V_\infty\cos\Lambda}\right) + \sum_{k=1}^{m}\left(\frac{c}{e}c_{m_{\delta_k}} + c_{L_{\delta_k}}\right)\delta_k\right]\right\} e q_\infty\cos^2\Lambda c - \rho g A e_{cg} + \rho I_{xx}\Theta_{tt} - \rho A e_{cg} W_{tt} \quad (34)$$

subject to fixed-end symmetric-mode boundary conditions $W(0,t) = W_x(0,t) = W_{xx}(L,t) = \frac{d}{dx}\left(EIW_{xx}(L,t) - EB_2\gamma'\Theta_x(L,t)\right) = 0$ and $\Theta(0,t) = \Theta_x(L,t) = 0$, whereupon the x-coordinate of the wing elastic axis is translated such that the wing root section is at $x = 0$ and wing tip section is at $x = L$.

These equations describe the wing bending and torsional deflections due to aerodynamic forces and moments. Using Galerkin's method,[7] the bending and torsional deflections can be approximated as

$$W(x,t) = \sum_{j=1}^{n} w_j(t)\,\Phi_j(x) \quad (35)$$

$$\Theta(x,t) = \sum_{j=0}^{n} \theta_j(t)\,\Psi_j(x) \tag{36}$$

where $w_j(t)$ and $\theta_j(t)$ are the generalized coordinates for static bending and torsion, and $\Phi_j(x)$ and $\Psi_j(x)$ are the assumed normalized eigenfunctions of the j-th bending and torsion aeroelastic modes, respectively, $j = 1, 2, \ldots, n$.

The normalized eigenfunctions are given by

$$\Phi_j(x) = \cosh(\beta_j x) - \cos(\beta_j x) - \frac{\cosh(\beta_j L) + \cos(\beta_j L)}{\sinh(\beta_j L) + \sin(\beta_j L)}\left[\sinh(\beta_j x) - \sin(\beta_j x)\right] \tag{37}$$

$$\Psi_j(x) = \sqrt{2}\sin\frac{(2j-1)\pi x}{2L} \tag{38}$$

where $\beta_j L = 1.87510, 4.69409, \ldots$ is the eigenvalue of the j-th bending mode of a uniform cantilever beam, and the eigenfunctions $\Phi_j(x)$ and $\Psi_j(x)$ satisfy the orthogonal condition

$$\int_0^L \Phi_i(x)\,\Phi_j(x)\,dx = \int_0^L \Psi_i(x)\,\Psi_j(x)\,dx = \begin{cases} L & i = j \\ 0 & i \neq j \end{cases} \tag{39}$$

The weak-form integral expressions of the dynamic aeroelastic equations are obtained by multiplying the bending and torsion aeroelastic equations by $\Phi_i(x)$ and $\Psi_i(x)$, and then integrating over the wing span. This yields

$$\begin{aligned}
&\sum_{j=1}^{n}\int_0^L \Phi_i \frac{d^2}{dx^2}\left(-EB_2\gamma'\theta_j\Psi_j' + EI_{yy}w_j\Phi_j''\right)dx = \\
&\sum_{j=1}^{n}\int_0^L \Phi_i\left[c_{L_0} + c_{L_\alpha}\left(\frac{\alpha}{\cos\Lambda} + \frac{qx_{ac}}{V_\infty\cos\Lambda} - w_j\Phi_j'\tan\Lambda - \theta_j\Psi_j - \frac{\dot{w}_j\Phi_j - e\dot{\theta}_j\Psi_j}{V_\infty\cos\Lambda}\right) + \sum_{k=1}^{m} c_{L_{\delta_k}}\delta_k\right] q_\infty\cos^2\Lambda c\,dx \\
&\qquad - \int_0^L \Phi_i\rho g A\,dx - \sum_{j=1}^{n}\int_0^L \Phi_i\rho A\ddot{w}_j\Phi_j\,dx + \sum_{j=1}^{n}\int_0^L \Phi_i\rho A e_{cg}\ddot{\theta}_j\Psi_j\,dx
\end{aligned} \tag{40}$$

$$\begin{aligned}
&\sum_{j=1}^{n}\int_0^L \Psi_i \frac{d}{dx}\left\{\left[GJ + EB_1\left(\gamma'\right)^2\right]\theta_j\Psi_j' - EB_2\gamma' w_j\Phi_j''\right\}dx = \\
&\sum_{j=1}^{n}\int_0^L \Psi_i\left\{\frac{c}{e}c_{m_{ac}} + \left[c_{L_0} + c_{L_\alpha}\left(\frac{\alpha}{\cos\Lambda} + \frac{qx_{ac}}{V_\infty\cos\Lambda} - w_j\Phi_j'\tan\Lambda - \theta_j\Psi_j - \frac{\dot{w}_j\Phi_j - e\dot{\theta}_j\Psi_j}{V_\infty\cos\Lambda}\right) + \sum_{k=1}^{m}\left(\frac{c}{e}c_{m_{\delta_k}} + c_{L_{\delta_k}}\right)\delta_k\right]\right\}\times \\
&\qquad \times e q_\infty\cos^2\Lambda c\,dx - \int_0^L \Psi_i\rho g A e_{cg}\,dx + \sum_{j=1}^{n}\int_0^L \Psi_i\rho I_{xx}\ddot{\theta}_j\Psi_j\,dx - \sum_{j=1}^{n}\int_0^L \Psi_i\rho A e_{cg}\ddot{w}_j\Phi_j\,dx
\end{aligned} \tag{41}$$

The expressions of the left hand sides can be integrated by parts as

$$\begin{aligned}
\int_0^L \Phi_i \frac{d^2}{dx^2}\left(-EB_2\gamma'\theta_j\Psi_j' + EI_{yy}w_j\Phi_j''\right)dx &= \Phi_i\frac{d}{dx}\left(-EB_2\gamma'\theta_j\Psi_j' + EI_{yy}w_j\Phi_j''\right)\Big|_0^L \\
&\quad - \Phi_i'\left(-EB_2\gamma'\theta_j\Psi_j' + EI_{yy}w_j\Phi_j''\right)\Big|_0^L + \int_0^L \Phi_i''\left(-EB_2\gamma'\bar{\theta}\Psi_j' + EI_{yy}w_j\Phi_j''\right)dx
\end{aligned} \tag{42}$$

$$\begin{aligned}
\int_0^L \Psi_i \frac{d}{dx}\left\{\left[GJ + EB_1\left(\gamma'\right)^2\right]\theta_j\Psi_j' - EB_2\gamma' w_j\Phi_j''\right\}dx &= \Psi_i\left\{\left[GJ + EB_1\left(\gamma'\right)^2\right]\theta_j\Psi_j' - EB_2\gamma' w_j\Phi_j''\right\}\Big|_0^L \\
&\quad - \int_0^L \Psi_i'\left\{\left[GJ + EB_1\left(\gamma'\right)^2\right]\theta_j\Psi_j' - EB_2\gamma' w_j\Phi_j''\right\}dx
\end{aligned} \tag{43}$$

Upon enforcing the zero boundary conditions at the two end points, the weak-form dynamic aeroelastic equations are obtained as

$$\sum_{j=1}^{n}\int_0^L \Phi_i''\left(-EB_2\gamma'\theta_j\Psi_j'+EI_{yy}w_j\Phi_j''\right)dx$$
$$-\sum_{j=1}^{n}\int_0^L \Phi_i\left[c_{L_0}+c_{L_\alpha}\left(\frac{\Delta\alpha}{\cos\Lambda}+\frac{qx_{ac}}{V_\infty\cos\Lambda}-w_j\Phi_j'\tan\Lambda-\theta_j\Psi_j-\frac{\dot{w}_j\Phi_j-e\dot{\theta}_j\Psi_j}{V_\infty\cos\Lambda}\right)+\sum_{k=1}^{m}c_{L_{\delta_k}}\delta_k\right]q_\infty\cos^2\Lambda c dx$$
$$+\sum_{j=1}^{n}\int_0^L \Phi_i\rho A\ddot{w}_j\Phi_j dx-\sum_{j=1}^{n}\int_0^L \Phi_i\rho Ae_{cg}\ddot{\theta}_j\Psi_j dx=-\int_0^L \Phi_i\rho gA dx \quad (44)$$

$$\sum_{j=1}^{n}\int_0^L \Psi_i'\left\{\left[GJ+EB_1\left(\gamma'\right)^2\right]\theta_j\Psi_j'-EB_2\gamma' w_j\Phi_j''\right\}dx$$
$$+\sum_{j=1}^{n}\int_0^L \Psi_i\left\{\frac{c}{e}c_{m_{ac}}+\left[c_{L_0}+c_{L_\alpha}\left(\frac{\Delta\alpha}{\cos\Lambda}+\frac{qx_{ac}}{V_\infty\cos\Lambda}-w_j\Phi_j'\tan\Lambda-\theta_j\Psi_j-\frac{\dot{w}_j\Phi_j-e\dot{\theta}_j\Psi_j}{V_\infty\cos\Lambda}\right)+\sum_{k=1}^{m}\left(\frac{c}{e}c_{m_{\delta_k}}+c_{L_{\delta_k}}\right)\delta_k\right]\right\}\times$$
$$\times eq_\infty\cos^2\Lambda c dx+\sum_{j=1}^{n}\int_0^L \Psi_i\rho I_{xx}\ddot{\theta}_j\Psi_j dx-\sum_{j=1}^{n}\int_0^L \Psi_i\rho Ae_{cg}\ddot{w}_j\Phi_j dx=\int_0^L \Psi_i\rho gAe_{cg}dx \quad (45)$$

These equations can be expressed as

$$\sum_{j=1}^{n}\left(m_{w_i\theta_j}\ddot{\theta}_j+m_{w_iw_j}\ddot{w}_j+c_{w_i\theta_j}\dot{\theta}_j+c_{w_iw_j}\dot{w}_j+k_{w_i\theta_j}\theta_j+k_{w_iw_j}w_j+h_{w_i\alpha}\alpha+h_{w_iq}q\right)=f_{w_i}+\sum_{k=1}^{m}g_{w_i\delta_k}\delta_k \quad (46)$$

$$\sum_{j=1}^{n}\left(m_{\theta_i\theta_j}\ddot{\theta}_j+m_{\theta_iw_j}\ddot{w}_j+c_{\theta_i\theta_j}\dot{\theta}_j+c_{\theta_iw_j}\dot{w}_j+k_{\theta_i\theta_j}\theta_j+k_{\theta_iw_j}w_j+h_{\theta_i\alpha}\alpha+h_{\theta_iq}q\right)=f_{\theta_i}+\sum_{k=1}^{m}g_{\theta_i\delta_k}\delta_k \quad (47)$$

where

$$m_{w_iw_j}=\int_0^L \rho A\Phi_i\Phi_j dx \quad (48)$$

$$m_{w_i\theta_j}=-\int_0^L \rho Ae_{cg}\Phi_i\Psi_j dx \quad (49)$$

$$m_{\theta_iw_j}=-\int_0^L \rho Ae_{cg}\Psi_i\Phi_j dx \quad (50)$$

$$m_{\theta_i\theta_j}=\int_0^L \rho I_{xx}\Psi_i\Psi_j dx \quad (51)$$

$$c_{w_iw_j}=\frac{1}{2}\rho_\infty V_\infty\int_0^L c_{L_\alpha}\cos\Lambda c\Phi_i\Phi_j dx \quad (52)$$

$$c_{w_i\theta_j}=-\frac{1}{2}\rho_\infty V_\infty\int_0^L c_{L_\alpha}ec\cos\Lambda\Phi_i\Psi_j dx \quad (53)$$

$$c_{\theta_iw_j}=-\frac{1}{2}\rho_\infty V_\infty\int_0^L c_{L_\alpha}ec\cos\Lambda\Psi_i\Phi_j dx \quad (54)$$

$$c_{\theta_i\theta_j}=\frac{1}{2}\rho_\infty V_\infty\int_0^L c_{L_\alpha}e^2c\cos\Lambda\Psi_i\Psi_j dx \quad (55)$$

$$k_{w_iw_j}=\int_0^L EI_{yy}\Phi_i''\Phi_j''dx+q_\infty\int_0^L c_{L_\alpha}c\tan\Lambda\cos^2\Lambda\Phi_i\Phi_j'dx \quad (56)$$

$$k_{w_i\theta_j}=-\int_0^L EB_2\gamma'\Phi_i''\Psi_j'dx+q_\infty\int_0^L c_{L_\alpha}c\cos^2\Lambda\Phi_i\Psi_j dx \quad (57)$$

$$k_{\theta_i w_j} = -\int_0^L EB_2 \gamma' \Psi_i' \Phi_j'' dx - q_\infty \int_0^L c_{L_\alpha} ec \tan\Lambda \cos^2\Lambda \Psi_i \Phi_j' dx \tag{58}$$

$$k_{\theta_i \theta_j} = \int_0^L \left[GJ + EB_1 \left(\gamma'\right)^2 \right] \Psi_i' \Psi_j' dx - q_\infty \int_0^L c_{L_\alpha} ec \cos^2\Lambda \Psi_i \Psi_j dx \tag{59}$$

$$h_{w_i \alpha} = -q_\infty \int_0^L c_{L_\alpha} c \cos\Lambda \Phi_i dx \tag{60}$$

$$h_{w_i q} = -\frac{1}{2}\rho_\infty V_\infty \int_0^L c_{L_\alpha} c x_{ac} \cos\Lambda \Phi_i dx \tag{61}$$

$$h_{\theta_i \alpha} = q_\infty \int_0^L c_{L_\alpha} ec \cos\Lambda \Psi_i dx \tag{62}$$

$$h_{\theta_i q} = \frac{1}{2}\rho_\infty V_\infty \int_0^L c_{L_\alpha} ec x_{ac} \cos\Lambda \Psi_i dx \tag{63}$$

$$f_{w_i} = q_\infty \int_0^L c_{L_0} c \cos^2\Lambda \Phi_i dx - \int_0^L \rho g A \Phi_i dx \tag{64}$$

$$f_{\theta_i} = -q_\infty \int_0^L \left(c_{m_{ac}} c + c_{L_0} e\right) c \cos^2\Lambda \Psi_i dx + \int_0^L \rho g A e_{cg} \Psi_i dx \tag{65}$$

$$g_{w_i \delta_k} = q_\infty \int_0^L c_{L_{\delta_k}} c \cos^2\Lambda \Phi_i dx \tag{66}$$

$$g_{\theta_i \delta_k} = -q_\infty \int_0^L \left(c_{m_{\delta_k}} c + c_{L_{\delta_k}} e\right) c \cos^2\Lambda \Psi_i dx \tag{67}$$

The resultant matrix equation is obtained as

$$M\ddot{x}_e + C\dot{x}_e + Kx_e + Hx_a = F + G\delta \tag{68}$$

where $x_e = \begin{bmatrix} w_1 & w_2 & \cdots & w_n & \theta_1 & \theta_2 & \cdots & \theta_n \end{bmatrix}^\top$ is an elastic state vector of the generalized coordinates, $x_a = \begin{bmatrix} \alpha & q \end{bmatrix}^\top$ is an aerodynamic state vector of the angle of attack and pitch rate, $\delta = \begin{bmatrix} \delta_1 & \delta_2 & \cdots & \delta_n \end{bmatrix}^\top$ is a control vector of the control surface deflections, M is the generalized mass matrix, C is the generalized damping matrix, K is the generalized stiffness, H is the generalized aerodynamic coupling matrix, and G is the generalized force derivative vector due to the flap and slat deflections.

The generalized damping matrix is comprised of both the structural damping and the aerodynamic damping. The structural damping matrix can be obtained from a modal analysis that transforms the generalized coordinates into the modal coordinates via the eigenvalue analysis.

Consider the zero-speed structural dynamic equations

$$\ddot{x}_e + M^{-1}C_s\dot{x}_e + M^{-1}K_s x_e = M^{-1}F \tag{69}$$

where C_s is the structural damping matrix, K_s is the structural stiffness matrix corresponding to the stiffness matrix K at zero speed, and F is the force vector.

Assuming that the eigenvalues of the matrix $M^{-1}K_s$ are positive real and distinct, then by the similarity transformation, the matrix $M^{-1}K_s$ can be decomposed as

$$M^{-1}K_s = X\Omega^2 X^{-1} \tag{70}$$

where X is the eigenvector matrix and $\Omega = \mathrm{diag}\left(\omega_1, \omega_2, \ldots, \omega_n\right)$ is the diagonal matrix whose elements are the frequencies of the structural modes.

Let $q = X^{-1}x_e$ be the modal coordinates, then the transformed structural dynamics equation can be obtained as

$$\ddot{q} + X^{-1}M^{-1}C_s X\dot{q} + \Omega^2 q = X^{-1}F \tag{71}$$

which can be expressed in the modal coordinates as

$$\ddot{q}_i + 2\zeta_i\omega_i\dot{q}_i + \omega_i^2 q_i = f_i \tag{72}$$

where ζ_i is the damping ratio of the i-th mode.

Let $\zeta = \mathrm{diag}\left(\zeta_1, \zeta_2, \ldots, \zeta_n\right)$ be the damping ratio diagonal matrix, then the structural damping matrix is computed as

$$C_s = 2MX\zeta\Omega X^{-1} \tag{73}$$

The total damping matrix includes both the structural damping matrix and the aerodynamic damping matrix according to

$$C = C_s + C_a \tag{74}$$

where C_a is the aerodynamic damping matrix whose elements are defined by $c_{\theta_i\theta_j}$, $c_{\theta_i w_j}$, $c_{w_i\theta_j}$, and $c_{w_i w_j}$.

The aeroelastic modes of the aeroelastic equations are then obtained by the eigenvalue analysis of the following system:

$$\begin{bmatrix} \dot{x}_e \\ \ddot{x}_e \end{bmatrix} = \begin{bmatrix} 0 & I \\ -M^{-1}K & -M^{-1}C \end{bmatrix} \begin{bmatrix} x_e \\ \dot{x}_e \end{bmatrix} + \begin{bmatrix} 0 \\ M^{-1}\left(G\delta - Hx_a\right) \end{bmatrix} \tag{75}$$

The flutter boundary is defined to be an airspeed at which the real parts of the eigenvalues of the systems become zero.

E. Aeroelastic Longitudinal Flight Dynamics

Due to the effect of aeroelasticity, the lift coefficient of an aircraft for symmetric flight can be expressed as

$$\begin{aligned} C_L(t) = {} & C_{L_0} + C_{L_\alpha}\alpha + C_{L_u}\left(\frac{V_\infty}{\bar{V}_\infty} - 1\right) + C_{L_q}\frac{q\bar{c}}{2\bar{V}_\infty} + C_{L_{\delta_e}}\delta_e + \sum_{k=1}^{m} C_{L_{\delta_k}}\delta_k \\ & + \sum_{j=1}^{n} C_{L_{w_j}}\frac{w_j(t)}{\bar{c}} + \sum_{j=1}^{n} C_{L_{\theta_j}}\theta_j(t) + \sum_{j=1}^{n} C_{L_{\dot{w}_j}}\frac{\dot{w}_j(t)}{\bar{V}_\infty} + \sum_{j=1}^{n} C_{L_{\dot{\theta}_j}}\frac{\dot{\theta}_j(t)\bar{c}}{2\bar{V}_\infty} \end{aligned} \tag{76}$$

where$\bar{c}$ is the mean aerodynamic chord, $\bar{V}_\infty$ is the trim airspeed, and $C_{L_{\theta_j}}$, $C_{L_{w_j}}$, $C_{L_{\dot{\theta}_j}}$, and $C_{L_{\dot{w}_j}}$ are the non-dimensional aeroelastic lift sensitivities or derivatives which are defined as

$$C_{L_{w_j}} = -\frac{2c_{L_\alpha}\bar{c}}{S}\int_0^L \tan\Lambda\cos^2\Lambda c\Phi_j' dx \tag{77}$$

$$C_{L_{\theta_j}} = -\frac{2c_{L_\alpha}}{S}\int_0^L \cos^2\Lambda c\Psi_j dx \tag{78}$$

$$C_{L_{\dot{w}_j}} = -\frac{2c_{L_\alpha}\bar{V}_\infty}{V_\infty S}\int_0^L \cos\Lambda c\Phi_j dx \tag{79}$$

$$C_{L_{\dot{\theta}_j}} = \frac{4c_{L_\alpha}\bar{V}_\infty}{V_\infty S\bar{c}}\int_0^L e\cos\Lambda c\Psi_j dx \tag{80}$$

The drag coefficient due to aeroelasticity may be modeled by a parabolic drag polar

$$C_D(t) = C_{D_0} + \frac{C_L^2(t)}{\pi AR\varepsilon} \tag{81}$$

where AR is the wing aspect ratio, and ε is the span efficiency factor.

In addition, the pitching moment coefficient of an aircraft is also influenced by the aeroelastic effects due to changes in wing lift characteristics. The pitching moment coefficient can be expressed as

$$\begin{aligned} C_m(t) = {} & C_{m_0} + C_{m_\alpha}\alpha + C_{m_u}\left(\frac{V_\infty}{\bar{V}_\infty} - 1\right) + C_{m_q}\frac{q\bar{c}}{2\bar{V}_\infty} + C_{m_{\delta_e}}\delta_e + \sum_{k=1}^{m} C_{m_{\delta_k}}\delta_k \\ & + \sum_{j=1}^{n} C_{m_{w_j}}\frac{w_j(t)}{\bar{c}} + \sum_{j=1}^{n} C_{m_{\theta_j}}\theta_j(t) + \sum_{j=1}^{n} C_{m_{\dot{w}_j}}\frac{\dot{w}_j(t)}{\bar{V}_\infty} + \sum_{j=1}^{n} C_{m_{\dot{\theta}_j}}\frac{\dot{\theta}_j(t)\bar{c}}{2\bar{V}_\infty} \end{aligned} \tag{82}$$

where $C_{m_{\theta_j}}$, $C_{m_{w_j}}$, $C_{m_{\dot{\theta}_j}}$, and $C_{m_{\dot{w}_j}}$ are the non-dimensional aeroelastic pitch moment sensitivities or derivatives

$$C_{m_{w_j}} = \frac{2c_{L_\alpha}}{S}\int_0^L x_{ac}\tan\Lambda\cos^2\Lambda c\Phi_j' dx \tag{83}$$

$$C_{m_{\theta_j}} = \frac{2c_{L_\alpha}}{S\bar{c}}\int_0^L x_{ac}\cos^2\Lambda c\Psi_j dx \tag{84}$$

$$C_{m_{\dot{w}_j}} = \frac{2c_{L_\alpha}\bar{V}_\infty}{V_\infty S\bar{c}}\int_0^L x_{ac}\cos\Lambda c\Phi_j dx \tag{85}$$

$$C_{m_{\dot{\theta}_j}} = -\frac{4c_{L_\alpha}\bar{V}_\infty}{V_\infty S\bar{c}^2}\int_0^L x_{ac}e\cos\Lambda c\Psi_j dx \tag{86}$$

The aircraft longitudinal dynamics in the stability axes with $\beta = 0$, $\phi = 0$, $p = 0$, and $r = 0$ are then described by

$$m\dot{V}_\infty = -C_D q_\infty S + T\cos\alpha - mg\sin(\theta - \alpha) \tag{87}$$

$$mV_\infty\dot{\alpha} = -C_L q_\infty S - T\sin\alpha + mg\cos(\theta - \alpha) \tag{88}$$

$$I_{YY}\dot{q} = C_m q_\infty S\bar{c} + \frac{Tz_e}{q_\infty S\bar{c}} \tag{89}$$

$$\dot{\theta} = q \tag{90}$$

where θ is the pitch attitude, S is the aircraft reference wing area, I_{YY} is the aircraft moment of inertia about the pitch axis, T is the thrust force, and z_e is the offset of the thrust line below the aircraft CG.

III. Aeroelastic Generic Transport Model

Consider the full-scale GTM[8] at a mid-point cruise condition of Mach 0.8 and 30,000 ft with 50% fuel remaining as shown in Figure 5.

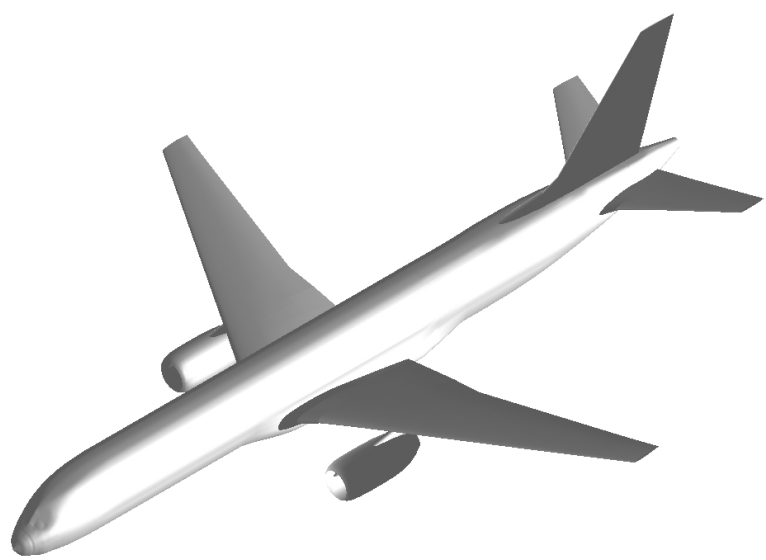

Figure 5 - Generic Transport Model

It is of interest to examine the effect of aeroelasticity on the short period mode of the aircraft. For simplicity, only the first bending mode (1B) and first torsion mode(1T) are considered. The coupled aeroelastic flight dynamic model of the GTM can be expressed in the following state space form:

$$
\begin{bmatrix} \dot{\alpha} \\ \dot{q} \\ \dot{w}_1 \\ \dot{\theta}_1 \\ \ddot{w}_1 \\ \ddot{\theta}_1 \end{bmatrix} =
\begin{bmatrix}
-\frac{1}{m_{\alpha\alpha}} C_{L_\alpha} & \frac{1}{m_{\alpha\alpha}} \left(\frac{m V_\infty}{q_\infty S} - \frac{C_{L_q} \bar{c}}{2 V_\infty} \right) & -\frac{1}{m_{\alpha\alpha}} \frac{C_{L_{w_1}}}{\bar{c}} & -\frac{1}{m_{\alpha\alpha}} C_{L_{\theta_1}} & -\frac{1}{m_{\alpha\alpha}} \frac{C_{L_{\dot{\theta}_1}} \bar{c}}{2 \bar{V}_\infty} \\
\frac{1}{m_{qq}} \left(C_{m_\alpha} + \frac{m_{q\alpha}}{m_{\alpha\alpha}} C_{L_\alpha} \right) & \frac{1}{m_{qq}} \left[\frac{C_{m_q} \bar{c}}{2 V_\infty} + \frac{m_{q\alpha}}{m_{\alpha\alpha}} \left(\frac{C_{L_q} \bar{c}}{2 V_\infty} - \frac{m V_\infty}{q_\infty S} \right) \right] & \frac{1}{m_{qq}} \left(\frac{C_{m_{w_1}}}{\bar{c}} + \frac{m_{q\alpha}}{m_{\alpha\alpha}} \frac{C_{L_{w_1}}}{\bar{c}} \right) & \frac{1}{m_{qq}} \left(C_{m_{\theta_1}} + \frac{m_{q\alpha}}{m_{\alpha\alpha}} C_{L_{\theta_1}} \right) & \frac{1}{m_{qq}} \left(\frac{C_{m_{\dot{\theta}_1}} \bar{c}}{2 \bar{V}_\infty} + \frac{m_{q\alpha}}{m_{\alpha\alpha}} \frac{C_{L_{\dot{\theta}_1}} \bar{c}}{2 \bar{V}_\infty} \right) \\
0 & 0 & 0 & 0 & 1 \\
0 & 0 & 0 & 0 & 0 \\
-\frac{1}{m_{w_1 w_1}} h_{w_1 \alpha} & -\frac{1}{m_{w_1 w_1}} h_{w_1 q} & -\frac{1}{m_{w_1 w_1}} k_{w_1 w_1} & -\frac{1}{m_{w_1 w_1}} k_{w_1 \theta_1} & -\frac{1}{m_{w_1 w_1}} c_{w_1 w_1} \\
-\frac{1}{m_{\theta_1 \theta_1}} h_{\theta_1 \alpha} & -\frac{1}{m_{\theta_1 \theta_1}} h_{\theta_1 q} & -\frac{1}{m_{\theta_1 \theta_1}} k_{\theta_1 w_1} & -\frac{1}{m_{\theta_1 \theta_1}} k_{\theta_1 \theta_1} & -\frac{1}{m_{\theta_1 \theta_1}} c_{\theta_1 w_1}
\end{bmatrix}
\begin{bmatrix} \alpha \\ q \\ w \\ \theta \\ \dot{w} \\ \dot{\theta} \end{bmatrix}
+
\begin{bmatrix}
-\frac{1}{m_{\alpha\alpha}} C_{L_{\delta_e}} & -\frac{1}{m_{\alpha\alpha}} C_{L_\delta} \\
\frac{1}{m_{qq}} \left(C_{m_{\delta_e}} + \frac{m_{q\alpha}}{m_{\alpha\alpha}} C_{L_{\delta_e}} \right) & \frac{1}{m_{qq}} \left(C_{m_\delta} + \frac{m_{q\alpha}}{m_{\alpha\alpha}} C_{L_\delta} \right) \\
0 & 0 \\
0 & 0 \\
0 & \frac{1}{m_{w_1 w_1}} g_{w_1 \delta_1} \\
0 & -\frac{1}{m_{w_1 w_1}} g_{\theta_1 \delta_1}
\end{bmatrix}
\begin{bmatrix} \delta_e \\ \delta_1 \end{bmatrix} \tag{91}
$$

where δ_1 is a symmetric control surface on the wing and $m_{\alpha\alpha}$, $m_{q\alpha}$, and m_{qq} are defined as

$$
m_{\alpha\alpha} = \frac{m \bar{V}_\infty}{q_\infty S} + \frac{C_{L_{\dot{\alpha}}} \bar{c}}{2 \bar{V}_\infty} \tag{92}
$$

$$
m_{q\alpha} = -\frac{C_{m_{\dot{\alpha}}} \bar{c}}{2 \bar{V}_\infty} \tag{93}
$$

$$
m_{qq} = \frac{I_{YY}}{q_\infty S \bar{c}} \tag{94}
$$

For the configuration with 50% fuel remaining and assuming a structural damping of $\zeta_1 = 0.1$, the A matrix is given by

$$
A = \begin{bmatrix}
-8.0134 \times 10^{-1} & 9.6574 \times 10^{-1} & 1.2608 \times 10^{-2} & 5.0966 \times 10^{-1} & 5.4634 \times 10^{-4} & -2.4249 \times 10^{-3} \\
-2.4526 \times 10^{0} & -9.1468 \times 10^{-1} & 4.6020 \times 10^{-2} & 2.1726 \times 10^{0} & 3.5165 \times 10^{-3} & -6.2222 \times 10^{-2} \\
0 & 0 & 0 & 0 & 1 & 0 \\
0 & 0 & 0 & 0 & 0 & 1 \\
1.4285 \times 10^{3} & 1.5869 \times 10^{1} & -3.1602 \times 10^{1} & -1.4029 \times 10^{3} & -2.4360 \times 10^{0} & 5.2088 \times 10^{0} \\
-3.9282 \times 10^{2} & -1.8923 \times 10^{0} & 5.6931 \times 10^{0} & -2.8028 \times 10^{2} & 3.2271 \times 10^{-1} & -6.1484 \times 10^{0}
\end{bmatrix}
$$

The eigenvalues of the rigid aircraft's short period mode can be computed from the 2 by 2 upper left matrix partition. These eigenvalues are stable

$$
\lambda_{SP} = -0.8580 \pm 1.5380i
$$

The eigenvalues of the 4 by 4 lower right matrix partition are for the 1B and 1T modes which are also stable

$$
\lambda_{1B} = -2.0955 \pm 8.2006i
$$

$$
\lambda_{1T} = -2.1967 \pm 15.1755i
$$

The eigenvalues of the aeroelastic aircraft are also stable, but with reduced damping in the 1T mode, as seen below

$$\lambda_{SP} = -0.5077 \pm 0.5229i$$

$$\lambda_{1B} = -3.1878 \pm 8.3789i$$

$$\lambda_{1T} = -1.4547 \pm 15.1728i$$

The computed frequencies and damping ratios of the short period mode, and the 1B and 1T modes for the GTM with 50% fuel remaining are shown in Table 1.

Mode	Short Period	1B	1T
Uncoupled Frequency, rad/sec	1.761	8.4641	15.3337
Coupled Frequency, rad/sec	0.7288	8.9648	15.2424
Uncoupled Damping Ratio	0.4872	0.2476	0.1433
Coupled Damping Ratio	0.6966	0.3556	0.0954

Table 1 - Aeroelastic GTM Frequencies and Damping Ratios at Mach 0.8 and 30,000 ft

The frequencies and damping ratios as a function of the airspeed at the same altitude of 30,000 ft are plotted in Figures 6 and 7. Generally, the frequencies of the short period mode and 1B mode increase with increasing the airspeed, while the frequency of the 1T mode decreases precipitously with increasing the airspeed. The divergence speed is the airspeed at which the torsion modal frequency becomes zero. The damping ratios for both the short period mode and 1B mode generally increase with increasing the airspeed. The damping ratio for the 1T mode increases with increasing the airspeed up to Mach 0.7, and thereafter decreases rapidly. The flutter speed is the airspeed at which the damping ratio of any modes becomes zero. It is apparent that the 1T mode would exhibit a zero damping at a flutter speed of about Mach 0.85. The low damping ratio of the 1T mode can be a problem for aircraft stability. Active feedback control can potentially help improve the stability margin of the aeroelastic modes.

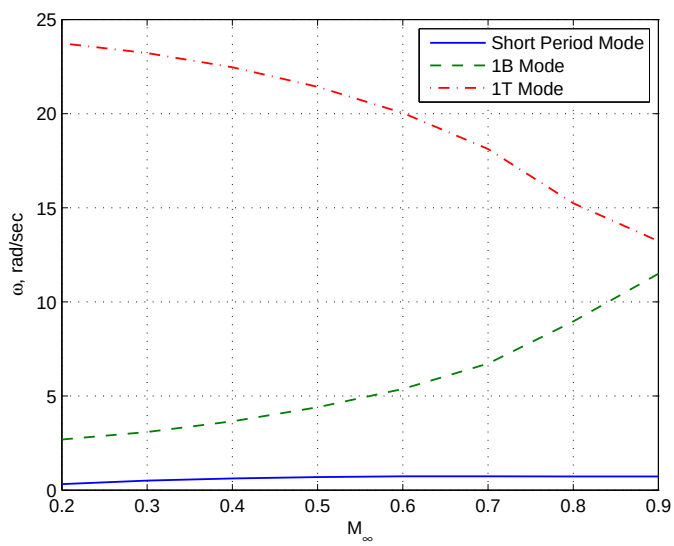

Figure 6 - Frequencies of Aircraft Modes

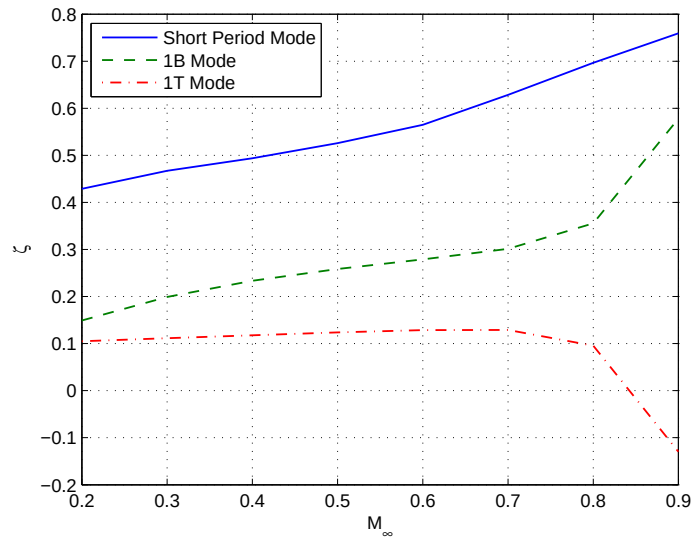

Figure 7 - Damping Ratios of Aircraft Modes

IV. Adaptive Control Application

Consider a linearized model of a flexible aircraft with matched uncertainty

$$\dot{x} = Ax + B\left[u - \Theta^{*\top}\Phi(x_r)\right] \tag{95}$$

$$x_r = Cx \tag{96}$$

where $x(t) : [0,\infty) \to \mathbb{R}^n$ is a state vector that is composed of a rigid-body state vector $x_r(t) : [0,\infty) \to \mathbb{R}^{n_r}$ and a flexible-body state vector $x_e(t) : [0,\infty) \to \mathbb{R}^{n_e = n - n_r}$, $u(t) : [0,\infty) \to \mathbb{R}^p$ is a control vector, $A \in \mathbb{R}^{n\times n}$ and $B \in \mathbb{R}^{n\times p}$ are constant and known matrices, and $\Theta^* \in \mathbb{R}^{m\times p}$ is a constant and unknown matrix that represents a matched parametric uncertainty in the rigid-body state, and $\Phi(x_r) : \mathbb{R}^{n_r} \to \mathbb{R}^m$ is a vector of known regressors.

The rigid-body dynamics with approximately zero-order flexible dynamics can be obtained by setting $\dot{x}_e = \varepsilon(x)$ where ε is a small parameter[7]

$$\begin{bmatrix} \dot{x}_r \\ \varepsilon \end{bmatrix} = \begin{bmatrix} A_{rr} & A_{re} \\ A_{er} & A_{ee} \end{bmatrix} \begin{bmatrix} x_r \\ x_e \end{bmatrix} + \begin{bmatrix} B_r \\ B_e \end{bmatrix} \left[u - \Theta^{*\top}\Phi(x_r)\right] \tag{97}$$

which yields

$$x_e = A_{ee}^{-1}\varepsilon(x) - A_{ee}^{-1}A_{er}x_r - A_{ee}^{-1}B_e\left[u - \Theta^{*\top}\Phi(x_r)\right]$$

Solving for x_e and substituting it into the rigid-body dynamics yields

$$\dot{x}_r = A_p x_r + B_p\left[u - \Theta^{*\top}\Phi(x_r)\right] - \Delta(x) \tag{98}$$

where

$$A_p = A_{rr} - A_{re}A_{ee}^{-1}A_{er} \tag{99}$$

$$B_p = B_r - A_{re}A_{ee}^{-1}B_e \tag{100}$$

$$\Delta(x) = -A_{re}A_{ee}^{-1}\varepsilon(x) \tag{101}$$

The term $\Delta(x)$ represents the effect of unmodeled flexible-body dynamics. The reduced-order plant matrix A_p is assumed to be Hurwitz.

The objective is to design an output-feedback adaptive control that enables the rigid-body state vector $x_r(t)$ to tracks a reference model

$$\dot{x}_m = A_m x_m + B_m r \tag{102}$$

where $A_m \in \mathbb{R}^{n_r \times n_r}$ is a known Hurwitz matrix and $B_m \in \mathbb{R}^{n_r \times r}$ is a known.matrix.

The controller is designed with

$$u = -K_x x_r + K_r r - \Theta^\top \Phi(x_r) \tag{103}$$

where $\Theta(t)$ is an estimate of Θ^* and it is assumed that K_x and K_r can be found such that the following model matching conditions are satisfied

$$A_p - B_p K_x = A_m \tag{104}$$

$$B_p K_r = B_m \tag{105}$$

Defining the tracking error as $e(t) = x_m(t) - x_r(t)$, then the tracking error equation becomes

$$\dot{e} = A_m e + B\tilde{\Theta}^\top \Phi(x_r) + \Delta(x) \tag{106}$$

where $\tilde{\Theta} = \Theta - \Theta^*$ is the estimation error.

Because of the presence of unmodeled dynamics, the standard model-reference adaptive law that adjusts $\Theta(t)$ which is given by

$$\dot{\Theta} = -\Gamma \Phi(x_r) e^\top PB \tag{107}$$

is not robust. As the adaptive gain Γ increases, the adaptive law becomes increasingly sensitive to the unmodeled dynamics $\Delta(x)$ that can lead to instability.[9]

To improve robustness to unmodeled dynamics, we use the optimal control modification adaptive law as proposed by Nguyen[1] to estimate the unknown parameter Θ^*. The optimal control modification adaptive law[1] is given by

$$\dot{\Theta} = -\Gamma \left[\Phi(x_r) e^\top PB - \nu \Phi(x_r) \Phi^\top(x_r) \Theta B^\top P A_m^{-1} B \right] \tag{108}$$

where $\Gamma = \Gamma^\top > 0 \in \mathbb{R}^{m \times m}$ is the adaptive gain, $\nu > 0 \in \mathbb{R}$ is a tuning parameter, and P is the solution of the Lyapunov equation

$$PA_m + A_m^\top P = -Q \tag{109}$$

As an alternative, the adaptive loop recovery adaptive law as proposed by Calise[2] can be used to adjust $\Theta(t)$ as follows:

$$\dot{\Theta} = -\Gamma \left[\Phi(x_r) e^\top PB + \eta \frac{d\Phi(x_r)}{dx_r} \frac{d\Phi^\top(x_r)}{dx_r} \Theta \right] \tag{110}$$

where $\eta > 0 \in \mathbb{R}$ is a tuning parameter.

Consider the aeroelastic GTM in the previous section, the reduced-order model of the rigid-body aircraft is given by

$$\begin{bmatrix} \dot{\alpha} \\ \dot{q} \end{bmatrix} = \begin{bmatrix} -0.2187 & 0.9720 \\ -0.4052 & -0.8913 \end{bmatrix} \begin{bmatrix} \alpha \\ q \end{bmatrix} + \begin{bmatrix} -0.0651 \\ -3.5277 \end{bmatrix} \left(\delta_e + \begin{bmatrix} \theta_\alpha^* & \theta_q^* \end{bmatrix} \begin{bmatrix} \alpha \\ q \end{bmatrix} \right) + \begin{bmatrix} \Delta_\alpha(\alpha, q, w, \theta, \dot{w}, \dot{\theta}) \\ \Delta_q(\alpha, q, w, \theta, \dot{w}, \dot{\theta}) \end{bmatrix} + \begin{bmatrix} f_\alpha(t) \\ f_q(t) \end{bmatrix}$$

where $\theta^* = 0.4$ and $\theta_q^* = -0.3071$ represent a parametric uncertainty corresponding to a short period frequency of 1.3247 rad/sec and a damping ratio of 0.0199 which is close to neutral pitch stability.

The time varying functions $f_\alpha(t)$ and $f_q(t)$ are disturbances due to a moderate vertical wind gust modeled by the Dryden turbulence model[10] with a vertical velocity amplitude of about 10 ft/sec and a pitch rate amplitude of 1.5 deg/sec as shown in Figure 8.

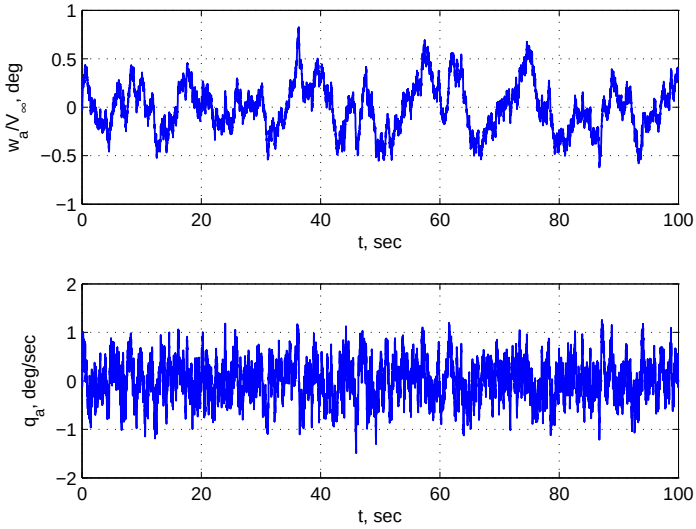

Figure 8 - Vertical Wind Gust Model

A desired reference model of the pitch attitude is given by

$$\ddot{\theta}_m + 2\zeta\omega_n\dot{\theta}_m + \omega_n^2\theta_m = \omega_n^2 r \tag{111}$$

where $\zeta = 0.85$ and $\omega_n = 1.5$ rad/sec are chosen to give a desired handling characteristic.

Let $x_r = \begin{bmatrix} \alpha & \theta & q \end{bmatrix}^\top$, $u = \delta_e$, and $\Theta^{*\top} = \begin{bmatrix} \theta_\alpha^* & 0 & \theta_q^* \end{bmatrix}$. A nominal controller is designed as $u_{nom} = -K_x x + k_r r$ where $K_x = \frac{1}{b_3}\begin{bmatrix} a_{31} & \omega_n^2 & 2\zeta\omega_n + a_{33} \end{bmatrix} = \begin{bmatrix} 0.1149 & -0.6378 & -0.4702 \end{bmatrix}$ and $k_r = \frac{1}{b_3}\omega_n^2 = -0.6378$. The closed-loop eigenvalues are -0.2112 and $-1.2750 \pm 0.7902i$. The nominal closed-loop plant is then chosen to be the reference model as

$$\underbrace{\begin{bmatrix} \dot{\alpha}_m \\ \dot{\theta}_m \\ \dot{q}_m \end{bmatrix}}_{\dot{x}_m} = \underbrace{\begin{bmatrix} -0.2112 & -0.0415 & 0.9414 \\ 0 & 0 & 1 \\ 0 & -2.2500 & -2.5500 \end{bmatrix}}_{A_m} \underbrace{\begin{bmatrix} \alpha_m \\ \theta_m \\ q_m \end{bmatrix}}_{x_m} + \underbrace{\begin{bmatrix} 0.0415 \\ 0 \\ 2.2500 \end{bmatrix}}_{B_m} r$$

The optimal control modification and the adaptive loop recovery adaptive laws are blended together in a combined adaptive law as follows:

$$\dot{\Theta} = -\Gamma\left[\Phi(x_r)\, e^\top PB - \nu\Phi(x_r)\,\Phi^\top(x_r)\,\Theta B^\top PA_m^{-1}B + \eta\frac{d\Phi(x_r)}{dx_r}\frac{d\Phi^\top(x_r)}{dx_r}\Theta\right] \tag{112}$$

where the adaptive gain is chosen to be $\Gamma = 100I$ and the input function is chosen as $\Phi(x_r) = \begin{bmatrix} 1 & \alpha & \theta & q \end{bmatrix}^\top$ whereby the bias input is used to handle the time-varying wind gust disturbances.

For the optimal control modification, the tuning parameters are set to $\nu = 0.2$ and $\eta = 0$. For the adaptive loop recovery, they are set to $\nu = 0$ and $\eta = 0.2$. Also the Jacobian of the input function $d\Phi(x_r)/dx_r$ is simply an identity matrix, thereby making the adaptive loop recovery effectively a σ-modification adaptive law.[11]

A pitch attitude doublet is commanded. The response of the aeroelastic GTM without adaptive control is plotted in Figure 9. It is clear that the aircraft response does not track well with the reference model.

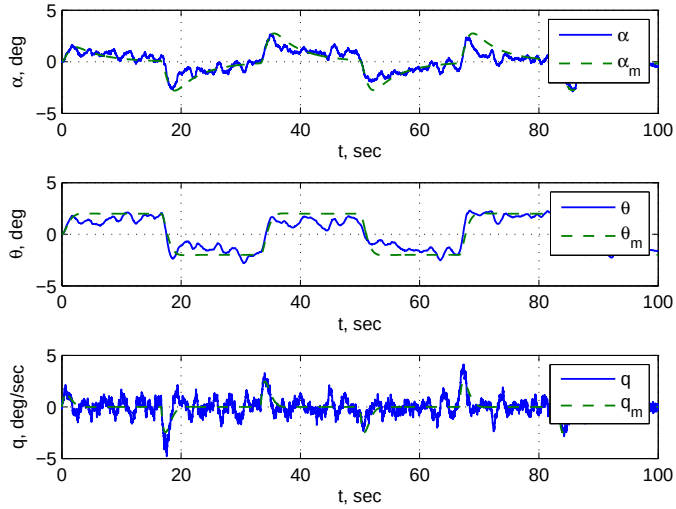

Figure 9 - Longitudinal Response of Aeroelastic GTM with No Adaptive Control

Using the standard model-reference adaptive control (MRAC) by setting $\nu = \eta = 0$, the pitch attitude tracking is much improved as shown in Figure 10. However, the initial transient in the pitch rate is quite large and is characterized by a high frequency signature. In contrast, with reference to Figure 11, the optimal control modification adaptive law is able to suppress the large initial transient of the pitch rate and the amplitude of the high frequency content. The response of the aircraft due to the adaptive loop recovery adaptive law as seen in Figure 12 is very much similar to the optimal control modification adaptive law.

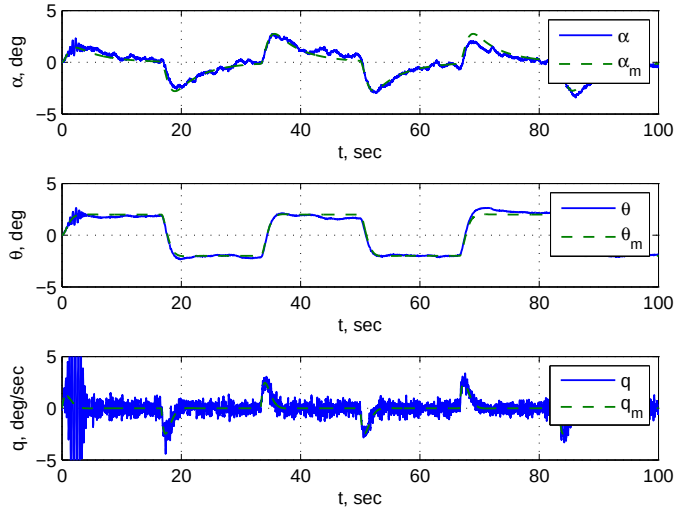

Figure 10 - Longitudinal Response of Aeroelastic GTM with Standard MRAC ($\Gamma = 100I$)

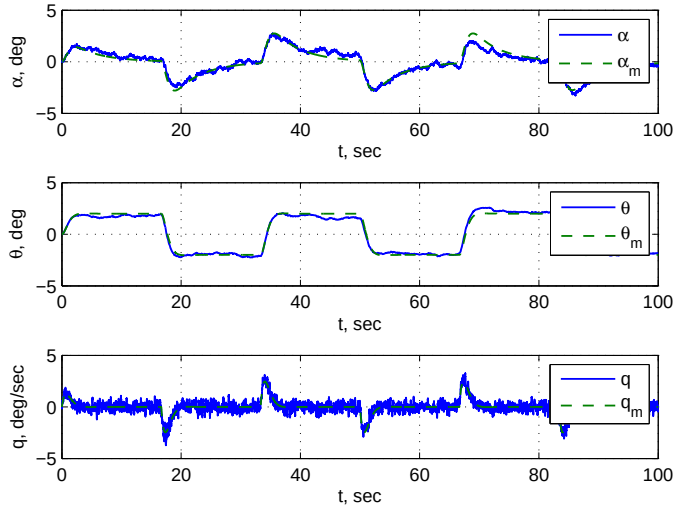

Figure 11 - Longitudinal Response of Aeroelastic GTM with Optimal Control Modification ($\Gamma = 100I$, $\nu = 0.2$)

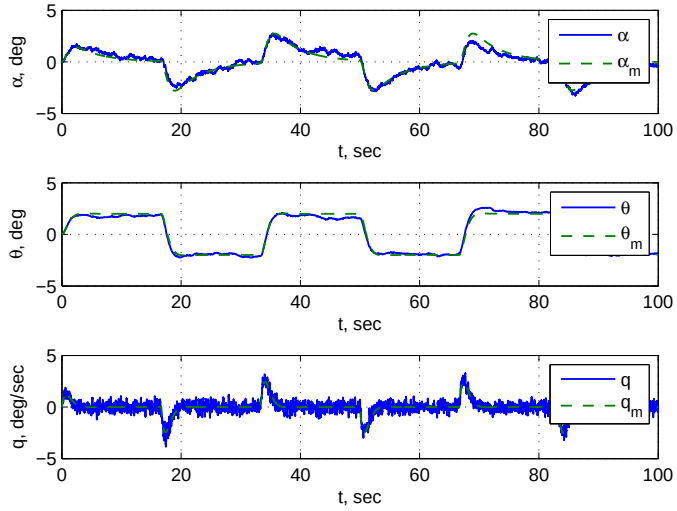

Figure 12 - Longitudinal Response of Aeroelastic GTM with Adaptive Loop Recovery ($\Gamma = 100I$, $\eta = 0.2$)

The aeroelastic wing tip bending and torsion deflections are shown in Figures 13 and 14 for four different controllers: baseline nominal control, standard MRAC, optimal control modification adaptive law, and adaptive loop recovery adaptive law. The aeroelastic GTM is modeled to be rather flexible to demonstrate the aeroelastic effects on adaptive control. The rigid-body pitch attitude command and wind gust result in a bending deflection amplitude of 5 ft and a torsional deflection amplitude of about 3 deg at the wing tip. The aeroelastic deflections are quite significant since the flight condition at Mach 0.8 is approaching the flutter speed at Mach 0.85. It is noted that the standard MRAC results in a very large initial transient of the torsional deflection. This large torsional deflection is clearly not realistic and in practice would result in excessive wing loading and wing stall. These effects are not taken into account in the simulations. Nonetheless, this illustrates the undesirable behavior of the standard MRAC in the flight control implementation for flexible aircraft.

Figure 15 is the plot of the elevator deflections for the four controllers. The standard MRAC produces a significant control saturation during the initial transient. This saturation leads to undesirable rigid-body aircraft response and aeroelastic deflections. Both the optimal control modification and adaptive loop recovery adaptive laws produce quite similar elevator deflections, although it is noted that the deflection is slightly greater in amplitude with the adaptive loop recovery adaptive law than with the optimal control modification adaptive law.

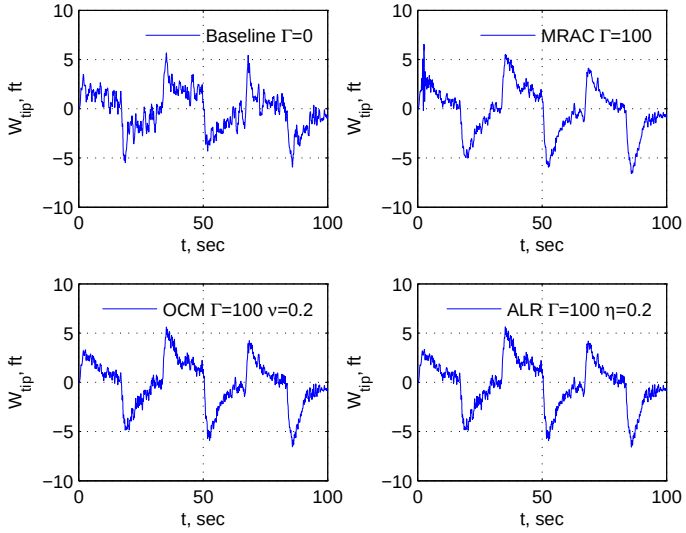

Figure 13 - Wing Tip Deflection of First Bending Mode

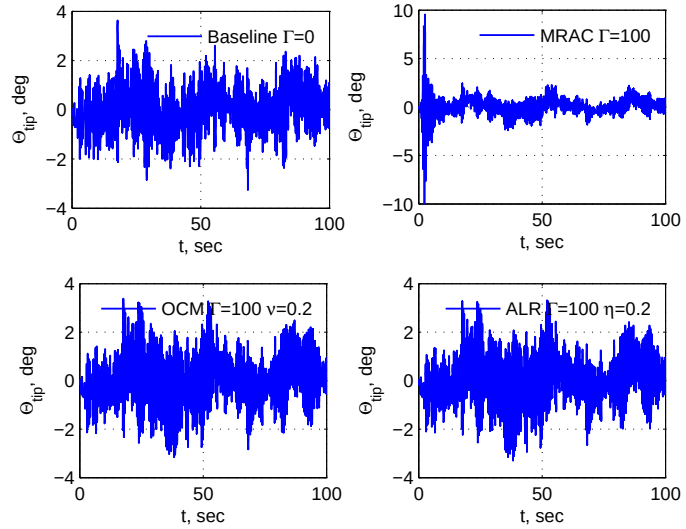

Figure 14 - Wing Tip Twist of First Torsion Mode

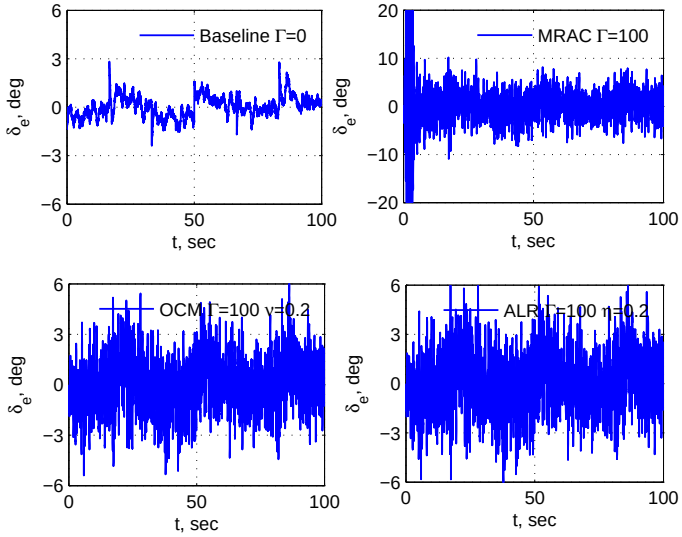

Figure 15 - Elevator Deflection

V. Conclusions

This paper presents an aeroelastic model of a generic transport model. Aeroelasticity theory is used to formulate a coupled bending torsion motion of the aircraft wing as a one-dimensional elastic member. The aeroelastic equations for the coupled bending torsion motion are solved by a weak-formed formulation using the Galerkin's method. The aeroelastic longitudinal dynamic model is then comprised of the longitudinal dynamic model of the rigid-body aircraft and the aeroelastic model of the flexible-body aircraft wing, both of which are coupled through the angle of attack and pitch rate. In general, as the airspeed increases, the torsional stiffness decreases, thereby causing the torsional frequencies to decrease. Moreover, as the airspeed becomes sufficiently fast, the damping ratio of the torsion mode decreases to zero, at which point a flutter speed is reached.

Adaptive control can be used to accommodate uncertainty for aeroelastic aircraft. An approach based on a reduced-order model is used to design adaptive controllers. The effect of aeroelasticity is captured in the reduced-order model as unmodeled dynamics. The standard model-reference adaptive control as well as two recently developed adaptive laws; optimal control modification and adaptive loop recovery, are implemented. Simulations include a moderate vertical wind gust Dryden's turbulence model. The results show that the standard MRAC is neither sufficiently robust nor able to produce well-behaved adaptive signals. Excessive torsional deflections and control saturation due to the standard MRAC are noted. Both the optimal control modification and adaptive loop recovery adaptive laws are seen to be more effective in reducing the tracking error while maintaining the aeroelastic deflections to within reasonable levels.

References

[1]Nguyen, N., Krishnakumar, K., and Boskovic, J., "An Optimal Control Modification to Model-Reference Adaptive Control for Fast Adaptation," AIAA Guidance, Navigation, and Control Conference, AIAA 2008-7283, August 2008.

[2]Calise, A. J., Yucelen, T., and Muse, J. A., "A Loop Recovery Method for Adaptive Control," AIAA Guidance, Navigation, and Control Conference, AIAA 2009-5967, August 2009.

[3]Hodges, D.H. and Pierce, G.A., *Introduction to Structural Dynamics and Aeroelasticity*, Cambridge University Press, 2002.

[4]Nguyen, N. T., "Integrated Flight Dynamic Modeling of Flexible Aircraft with Inertial Force-Propulsion-Aeroelastic Coupling," AIAA-2008-194, 46th AIAA Aerospace Sciences Meeting, Reno, NV, Jan 2008.

[5]Houbolt, J. C. and Brooks, G. W., "Differential Equations of Motion for Combined Flapwise Bending, Chordwise Bending, and Torsion of Twisted Nonuniform Rotor Blades," NACA Technical Note 3905, February 1957.

[6]Theodorsen, T. and Garrick, I.E., "Mechanism of Flutter - a Theoretical and Experimental Investigation of the Flutter Problem", NACA Report 685, 1940.

[7]Tuzcu, I., Nguyen, N., "Aeroelastic Modeling and Adaptive Control of Generic Transport Model," AIAA Atmospheric Flight Mechanics, AIAA-2010-7503, August 2010.

[8]Jordan, T. L., Langford, W. M., Belcastro, C. M., Foster, J. M., Shah, G. H., Howland, G., and Kidd, R., "Development of a Dynamically Scaled Generic Transport Model Testbed for Flight Research Experiments," AUVSI Unmanned Unlimited, Arlington, VA, 2004.

[9]Rohrs, C.E., Valavani, L., Athans, M., and Stein, G., "Robustness of Continuous-Time Adaptive Control Algorithms in the Presence of Unmodeled Dynamics," IEEE Transactions on Automatic Control, Vol AC-30, No. 9, pp. 881-889, 1985.

[10]Schmidt, L. V., *Introduction to Aircraft Flight Dynamics*, AIAA Education Series, 1998.

[11]Ioannu, P.A. and Sun, J., *Robust Adaptive Control*, Prentice-Hall, 1996.